DE GRUYTER OPEN

CIVIL AND ENVIRONMENTAL ENGINEERING REPORTS

ISSN 2080-5187

CEER 2016; 20 (1): 101-133
DOI: 10.1515/ceer-2016-0010

Original Research Article

NUMERICAL NON-EQUILIBRIUM AND SMOOTHING OF SOLUTIONS IN THE DIFFERENCE METHOD FOR PLANE 2-DIMENSIONAL ADHESIVE JOINTS

Piotr RAPP[1]
Poznan Uniwersity of Technology, Poland

Abstract

The subject of the paper is related to problems with numerical errors in the finite difference method used to solve equations of the theory of elasticity describing 2-dimensional adhesive joints in the plane stress state. Adhesive joints are described in terms of displacements by four elliptic partial differential equations of the second order with static and kinematic boundary conditions. If adhesive joint is constrained as a statically determinate body and is loaded by a self-equilibrated loading, the finite difference solution is sensitive to kinematic boundary conditions. Displacements computed at the constraints are not exactly zero. Thus, the solution features a numerical error as if the adhesive joint was not in equilibrium. Herein this phenomenon is called *numerical non-equilibrium*. The disturbances in displacements and stress distributions can be decreased or eliminated by a correction of loading acting on the adhesive joint or by *smoothing of solutions* based on Dirichlet boundary value problem.

Keywords: adhesive joint, equations of linear theory of elasticity, finite difference method, numerical error, smoothing of solutions, Dirichlet boundary value problem

1. MODEL OF 2-DIMENSIONAL ADHESIVE JOINT

An adhesive joint is considered as an assembly of two plane adherends connected along a common surface by an adhesive. It is assumed that the

[1] Corresponding author: Poznan Uniwersity of Technology, 5 M. Skłodowskiej-Curie Sq., 60-965 Poznań, Poland, e-mail: piotr.rapp@put.poznan.pl, tel .+48616652094

adherends are thin and have constant or moderately varying thickness. The adhesive is thin and may be of constant or moderately varying thickness, too. The adherend is considered thin when the ratio between its thickness and the dimension along the loading line of action does not exceed 0.1. A moderate variation of thickness is observed when the absolute value of the first derivative of thickness function does not exceed 0.2. Thickness of a plane element is measured perpendicularly to the plane 0XY. The joint thickness is measured in the direction normal to its mid-surface.

The joint is modelled as a plane 2-dimensional element parallel to the plane 0XY in a Cartesian set of co-ordinates. Projections of the adherends and the adhesive in the plane 0XY form the same figure of an arbitrary shape. Loading acting on the adhesive joint can be in the form of the forces parallel to the plane 0XY distributed on the surfaces and edges of adherends (Fig. 1).

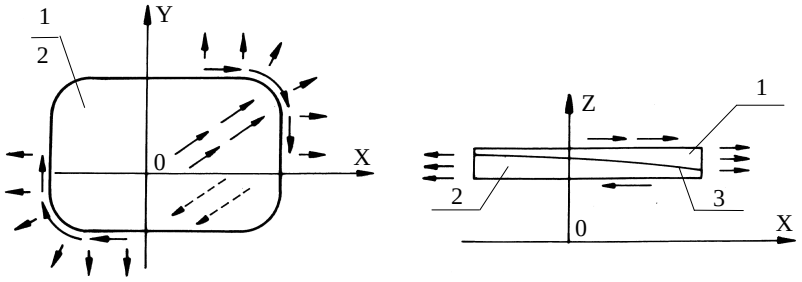

Fig. 1. Layout of an adhesive joint. 1 - adherend 1, 2 - adherend 2, 3 - adhesive

It is assumed that the flexural and torsional effects at plane adherends are of secondary order and can be neglected. Thus, the distribution of stresses across the adherend thickness is assumed to be constant and the stresses in adherends form plane states parallel to the plane 0XY.

An assumed layout of an adhesive joint is presented in Fig. 1. Thickness of adherends is described by functions $g_1 = g_1(x, y)$ and $g_2 = g_2(x, y)$, which are C^1-continuous in the sense of partial derivatives with respect to the variables x, y. The functions g_1 and g_2 can have zero values at some regions or in the vicinity of certain points on adherend edges.

The mid-plane of the adhesive is described by a function $s = s(x, y)$, which is C^1-continuous in the sense of partial derivatives with respect to the variables x, y. The thickness $t = t(x, y)$ of the adhesive is larger than zero in the entire domain and is C^1-continuous in the sense of partial derivatives with respect to the variables x, y.

The adhesive is modelled as an isotropic linearly-elastic medium with the material constants: Young's modulus E_s, shear modulus G_s and Poisson's ratio v_s, where $E_s = 2(1 + v_s)G_s$. The adhesive is subjected to stresses $\tau_x = \tau_x(x, y)$,

$\tau_y = \tau_y(x,y)$ tangent to its mid-plane and the stress $\sigma_N = \sigma_N(x,y)$ normal to it. It is assumed that the stresses are constant across the adhesive thickness. The action of the shear stresses τ_x and τ_y in the adhesive leads to a shear strain, which results in relative displacements of adhesive layers in directions tangent to the adhesive mid-plane. The stress σ_N results in an axial strain normal to the adhesive mid-plane. The assumptions regarding loading of the adhesive joint by forces parallel to the plane 0XY and concerning plane stress states in the adherends parallel to the plane 0XY, lead to the conclusion that the resultant from the stresses τ_x, τ_y and σ_N is also parallel to the plane 0XY.

Displacements in the adherends 1 and 2 are described by the functions $u_1 = u_1(x,y)$ and $u_2 = u_2(x,y)$ for the direction X and the functions $v_1 = v_1(x,y)$ and $v_2 = v_2(x,y)$ for the direction Y. The functions u_1, u_2, v_1, v_2 are C^2-continuous in the sense of partial derivatives with respect to the variables x, y.

Loading distributed at external surfaces of the adherends 1 and 2 are given in terms of components parallel to the axes X and Y and are described as $q_{1x} = q_{1x}(x,y)$, $q_{2x} = q_{2x}(x,y)$ and $q_{1y} = q_{1y}(x,y)$, $q_{2y} = q_{2y}(x,y)$. Orientations of the axes X and Y determine a positive sign of the loading functions.

The adherends 1 and 2 are bounded by circumferential edge surfaces (edges) perpendicular to the plane. The width of the edge surfaces is equal to the adherend thickness. If the width of the edge surface is larger than zero, than the edge is called *unsharp*. Stresses acting on unsharp edges of an adherend k are denoted by p_{kx} and p_{ky} (k = 1, 2). It is assumed that the stresses p_{kx} and p_{ky} are parallel to the axes X and Y, respectively, and are constant across the adherend thickness. These stresses are treated as a given external loading acting on the adherends in the plane parallel to 0XY. The width of the edge surface at a particular adherend or its fragment can be equal to zero. In such a case the edge is called *sharp*. Edge loading is not defined at sharp edges.

In the following, the displacement functions u_1, u_2, v_1, v_2 for the adherends are considered as unknown quantities and equations of the theory of elasticity in the plane stress state with boundary conditions are formulated for them. Knowing the displacement functions u_1, u_2, v_1, v_2 one can determine complete stress and strain states for adhesive and adherends.

2. GENERAL DISPLACEMENT EQUATIONS FOR ADHESIVE JOINT AND BOUNDARY CONDITIONS

It is assumed that adherends are made from orthotropic materials with principal axes of orthotropy coinciding with the axes X and Y of a co-ordinate system. An orthotropic material in the plane stress is described by five material constants: two moduli of longitudinal deformation E_{kx}, E_{ky}, one modulus of

shear deformation G_{kxy} and two Poisson's ratios v_{kxy}, v_{kyx}. It is assumed that the condition $\nu_{kxy}E_{kx} = \nu_{kyx}E_{ky}$ holds.

General equations of the theory of elasticity and boundary conditions for an adhesive joint in terms of displacements were derived in [18, 19, 20]. They read:

$$\left(\alpha_{1x}\frac{\partial^2 u_1}{\partial x^2}+\frac{\partial^2 u_1}{\partial y^2}+\beta_{1x}\frac{\partial^2 \upsilon_1}{\partial x\partial y}\right)g_1+\left(\alpha_{1x}\frac{\partial u_1}{\partial x}+(\beta_{1x}-1)\frac{\partial \upsilon_1}{\partial y}\right)\frac{\partial g_1}{\partial x}+$$
$$+\left(\frac{\partial u_1}{\partial y}+\frac{\partial \upsilon_1}{\partial x}\right)\frac{\partial g_1}{\partial y}-\gamma_{1u}(u_1-u_2)-\gamma_{1u\upsilon}(\upsilon_1-\upsilon_2)+\frac{q_{1x}}{G_{1xy}}=0, \tag{1.a}$$

$$\left(\frac{\partial^2 \upsilon_1}{\partial x^2}+\alpha_{1y}\frac{\partial^2 \upsilon_1}{\partial y^2}+\beta_{1y}\frac{\partial^2 u_1}{\partial x\partial y}\right)g_1+\left(\frac{\partial u_1}{\partial y}+\frac{\partial \upsilon_1}{\partial x}\right)\frac{\partial g_1}{\partial x}+$$
$$+\left((\beta_{1y}-1)\frac{\partial u_1}{\partial x}+\alpha_{1y}\frac{\partial \upsilon_1}{\partial y}\right)\frac{\partial g_1}{\partial y}-\gamma_{1uu}(u_1-u_2)-\gamma_{1\upsilon}(\upsilon_1-\upsilon_2)+\frac{q_{1y}}{G_{1xy}}=0, \tag{1.b}$$

$$\left(\alpha_{2x}\frac{\partial^2 u_2}{\partial x^2}+\frac{\partial^2 u_2}{\partial y^2}+\beta_{2x}\frac{\partial^2 \upsilon_2}{\partial x\partial y}\right)g_2+\left(\alpha_{2x}\frac{\partial u_2}{\partial x}+(\beta_{2x}-1)\frac{\partial \upsilon_2}{\partial y}\right)\frac{\partial g_2}{\partial x}+$$
$$+\left(\frac{\partial u_2}{\partial y}+\frac{\partial \upsilon_2}{\partial x}\right)\frac{\partial g_2}{\partial y}+\gamma_{2u}(u_1-u_2)+\gamma_{2u\upsilon}(\upsilon_1-\upsilon_2)+\frac{q_{2x}}{G_{2xy}}=0, \tag{1.c}$$

$$\left(\frac{\partial^2 \upsilon_2}{\partial x^2}+\alpha_{2y}\frac{\partial^2 \upsilon_2}{\partial y^2}+\beta_{2y}\frac{\partial^2 u_2}{\partial x\partial y}\right)g_2+\left(\frac{\partial u_2}{\partial y}+\frac{\partial \upsilon_2}{\partial x}\right)\frac{\partial g_2}{\partial x}+$$
$$+\left((\beta_{2y}-1)\frac{\partial u_2}{\partial x}+\alpha_{2y}\frac{\partial \upsilon_2}{\partial y}\right)\frac{\partial g_2}{\partial y}+\gamma_{2u}(u_1-u_2)+\gamma_{2\upsilon}(\upsilon_1-\upsilon_2)+\frac{q_{2y}}{G_{2xy}}=0, \tag{1.d}$$

where $k = 1$ for the adherend 1 and $k = 2$ for the adherend 2.

In the equations (1.a) – (1.d) the following notation was introduced:

$$\alpha_{kx}=\frac{E_{kx}}{G_{kxy}(1-\nu_{kxy}\nu_{kyx})}, \qquad \alpha_{ky}=\frac{E_{ky}}{G_{kxy}(1-\nu_{kxy}\nu_{kyx})}, \tag{2}$$

$$\beta_{kx}=1+\alpha_{kx}\nu_{kxy}, \qquad \beta_{ky}=1+\alpha_{ky}\nu_{kyx}, \tag{3}$$

$$\gamma_{ku}=\frac{\sqrt{1-\sin^2\varphi_x\sin^2\varphi_y}}{G_{kxy}\cos\varphi_x\cos\varphi_y}\cdot\frac{G_s}{t}\cdot\delta_u, \qquad \gamma_{k\upsilon}=\frac{\sqrt{1-\sin^2\varphi_x\sin^2\varphi_y}}{G_{kxy}\cos\varphi_x\cos\varphi_y}\cdot\frac{G_s}{t}\cdot\delta_\upsilon, \tag{4.a}$$

$$\gamma_{ku\upsilon}=\frac{\sqrt{1-\sin^2\varphi_x\sin^2\varphi_y}}{G_{kxy}\cos\varphi_x\cos\varphi_y}\cdot\frac{G_s}{t}\cdot\delta_{u\upsilon},\qquad \gamma_{kuu}=\frac{\sqrt{1-\sin^2\varphi_x\sin^2\varphi_y}}{G_{kxy}\cos\varphi_x\cos\varphi_y}\cdot\frac{G_s}{t}\cdot\delta_{uu},\tag{4.b}$$

$$\delta_u=\frac{\dfrac{1}{\cos^2\varphi_x}+\sin^2\varphi_y\tan^2\varphi_x+\dfrac{G_s}{E_s}(1-\sin^2\varphi_x\sin^2\varphi_y)\tan^2\varphi_y}{1+\dfrac{G_s}{E_s}\left((1+\sin^2\varphi_y)\tan^2\varphi_x+(1+\sin^2\varphi_x)\tan^2\varphi_y\right)},\tag{5.a}$$

$$\delta_{u\upsilon}=\delta_{uu}=\frac{\left(2-\dfrac{G_s}{E_s}(1-\sin^2\varphi_x\sin^2\varphi_y)\right)\tan\varphi_x\tan\varphi_y}{1+\dfrac{G_s}{E_s}\left((1+\sin^2\varphi_y)\tan^2\varphi_x+(1+\sin^2\varphi_x)\tan^2\varphi_y\right)},\tag{5.b}$$

$$\delta_\upsilon=\frac{\dfrac{1}{\cos^2\varphi_y}+\sin^2\varphi_x\tan^2\varphi_y+\dfrac{G_s}{E_s}(1-\sin^2\varphi_x\sin^2\varphi_y)\tan^2\varphi_x}{1+\dfrac{G_s}{E_s}\left((1+\sin^2\varphi_y)\tan^2\varphi_x+(1+\sin^2\varphi_x)\tan^2\varphi_y\right)}.\tag{5.c}$$

The angles φ_x, φ_y are given by the formulae: $\tan\varphi_x=-\partial s/\partial x$ and $\tan\varphi_y=-\partial s/\partial y$, where $s=s(x,y)$ is the equation of the mid-plane of adhesive in the co-ordinate system 0XYZ.

The equations (1.a) – (1.d) form a set of four partial differential equations of the second order in terms of displacements describing an adhesive joint between adherends with varying thickness made from orthotropic materials and with an adhesive defined by a curved surface. The unknown functions are the displacements $u_1, u_2, \upsilon_1, \upsilon_2$ for the adherends 1 and 2. It can be shown [18], that the characteristic form of the main part of the equations set (1.a) – (1.d) is positively definite. Hence the set (1.a) – (1.d) is elliptic. Thus, existence and uniqueness of solution to the set (1.a) – (1.d) with appropriate boundary conditions are ensured [5, 7, 9, 10, 13, 15, 22].

Static boundary conditions for adherends displacements at unsharp edges take the form:

$$\left(\alpha_{1x}\frac{\partial u_1}{\partial x}+(\beta_{1x}-1)\frac{\partial \upsilon_1}{\partial y}\right)\cdot l+\left(\frac{\partial u_1}{\partial y}+\frac{\partial \upsilon_1}{\partial x}\right)\cdot m=\frac{p_{1x}}{G_{1xy}},\tag{6.a}$$

$$\left(\frac{\partial u_1}{\partial y}+\frac{\partial \upsilon_1}{\partial x}\right)\cdot l+\left((\beta_{1y}-1)\frac{\partial u_1}{\partial x}+\alpha_{1y}\frac{\partial \upsilon_1}{\partial y}\right)\cdot m=\frac{p_{1y}}{G_{1xy}}, \tag{6.b}$$

$$\left(\alpha_{2x}\frac{\partial u_2}{\partial x}+(\beta_{2x}-1)\frac{\partial \upsilon_2}{\partial y}\right)\cdot l+\left(\frac{\partial u_2}{\partial y}+\frac{\partial \upsilon_2}{\partial x}\right)\cdot m=\frac{p_{2x}}{G_{2xy}}, \tag{6.c}$$

$$\left(\frac{\partial u_2}{\partial y}+\frac{\partial \upsilon_2}{\partial x}\right)\cdot l+\left((\beta_{2y}-1)\frac{\partial u_2}{\partial x}+\alpha_{2y}\frac{\partial \upsilon_2}{\partial y}\right)\cdot m=\frac{p_{2y}}{G_{2xy}}, \tag{6.d}$$

where l and m denote directional cosines of a vector normal to adherend edges. Boundary conditions at sharp edges read:

$$\left(\alpha_{1x}\frac{\partial u_1}{\partial x}+(\beta_{1x}-1)\frac{\partial \upsilon_1}{\partial y}\right)\frac{\partial g_1}{\partial x}+\left(\frac{\partial u_1}{\partial y}+\frac{\partial \upsilon_1}{\partial x}\right)\frac{\partial g_1}{\partial y}-\gamma_{1u}(u_1-u_2)-\gamma_{1u\upsilon}(\upsilon_1-\upsilon_2)+\frac{q_{1x}}{G_{1xy}}=0, \tag{7.a}$$

$$\left(\frac{\partial u_1}{\partial y}+\frac{\partial \upsilon_1}{\partial x}\right)\frac{\partial g_1}{\partial x}+\left((\beta_{1y}-1)\frac{\partial u_1}{\partial x}+\alpha_{1y}\frac{\partial \upsilon_1}{\partial y}\right)\frac{\partial g_1}{\partial y}-\gamma_{1u}(u_1-u_2)-\gamma_{1\upsilon}(\upsilon_1-\upsilon_2)+\frac{q_{1y}}{G_{1xy}}=0, \tag{7.b}$$

$$\left(\alpha_{2x}\frac{\partial u_2}{\partial x}+(\beta_{2x}-1)\frac{\partial \upsilon_2}{\partial y}\right)\frac{\partial g_2}{\partial x}+\left(\frac{\partial u_2}{\partial y}+\frac{\partial \upsilon_2}{\partial x}\right)\frac{\partial g_2}{\partial y}+\gamma_{2u}(u_1-u_2)+\gamma_{2u\upsilon}(\upsilon_1-\upsilon_2)+\frac{q_{2x}}{G_{2xy}}=0, \tag{7.c}$$

$$\left(\frac{\partial u_2}{\partial y}+\frac{\partial \upsilon_2}{\partial x}\right)\frac{\partial g_2}{\partial x}+\left((\beta_{2y}-1)\frac{\partial u_2}{\partial x}+\alpha_{2y}\frac{\partial \upsilon_2}{\partial y}\right)\frac{\partial g_2}{\partial y}+\gamma_{2u}(u_1-u_2)+\gamma_{2\upsilon}(\upsilon_1-\upsilon_2)+\frac{q_{2y}}{G_{2xy}}=0. \tag{7.d}$$

The boundary conditions (7.a) – (7.d) for sharp edges are identical with the equations (1.a) – (1.d), with $g_1 = g_2 = 0$ substituted.

Boundary conditions at both unsharp and sharp edges represent equilibrium conditions, however the character of equilibrium is different in these two cases.

The boundary conditions at an unsharp edge express equilibrium of internal stresses in an adherend and external stresses representing adherend loading. Thus, the equations (1.a) – (1.d) at an unsharp edge preserve their form and an unsharp edge belongs to the definition set for these equations. The equations (1.a) – (1.d) for a sharp edge degenerate to the form (7.a) – (7.d) and, in order to avoid a singularity, a sharp edge has to be excluded from the definition set of the equations (1.a) – (1.d). The values of displacements and their derivatives

present in the conditions (7.a) – (7.d) have to be considered as unilateral internal limits.

In the theory of differential equations the boundary conditions representing equilibrium conditions in terms of derivatives of the unknown functions are called *natural boundary conditions*. In mechanics the term *static boundary conditions* is used.

In the displacement formulation static boundary conditions are not sufficient to obtain a unique solution for the equations (1.a) – (1.d). Indeed, if the functions $u_k(x,y)$ and $v_k(x,y)$ are solutions to the equations (1.a) – (1.d), then for arbitrary constants u_0 , v_0 , θ the functions

$$u_k(x,y) - \theta \cdot y + u_0, \quad v_k(x,y) + \theta \cdot x + v_0$$

(k = 1, 2) are solutions, too. It can be verified by a simple substitution. The constants u_0 and v_0 are interpreted as arbitrary translations of the adhesive joint in the directions of the axes X and Y, while θ is interpreted as a small rotation of the adhesive joint about the origin 0 of the co-ordinate set 0XY.

Thus, it can be concluded that the adhesive joint has three degrees of freedom in the class of solutions to the equations (1.a) – (1.d): two as a mechanism with respect to two arbitrary translations along the axes X and Y and one as a mechanism with respect to a small rotation about the origin 0 of the co-ordinate set 0XY.

In order to ensure uniqueness of a solution to the equations (1.a) – (1.d) one has to constrain the displacements with respect to these three degrees of freedom, and to obtain a geometrically stable system. For instance:

$$u_k(0,0) = 0, \; v_k(0,0) = 0, \quad v_k(x_q,0) = 0, \text{ where } x_q \neq 0 \tag{8}$$

or

$$u_k(0,0) = 0, \; v_k(0,0) = 0, \quad u_k(0,y_q) = 0, \text{ where } y_q \neq 0, \tag{9}$$

with k = 1 or k = 2. Such a constraint set or any equivalent one is statically determinate and support reactions at the constraints can be uniquely determined. If an adhesive joint is loaded by a self-equilibrated set of forces and it is constrained in a statically determinate way, then support reactions at the constraints are zero. Stress and strain states in this case do not depend on the way of constraining. In the case of an adhesive joint loaded by a given self-equilibrated loading and constrained in a statically determinate way, displacements for various constraining layout differ by a translation and rotation as in the case of a rigid body.

The constraint points leading to a geometric stability of the system have to be considered as boundary points. An adhesive joint can be constrained in a more

complex way, to make it statically indeterminate by imposing appropriate constraints on its adherends. In particular one can constrain some points or impose displacement for at entire edges of adherends. Such boundary conditions in the theory of differential equations are called as *essential boundary conditions* or *Dirichlet boundary conditions.* In mechanics the boundary conditions imposed on displacements are called *kinematic boundary conditions.*

3. FORMULAE EXPRESSING STRESSES IN ADHESIVE AND ADHERENDS

Having found the functions of displacements $u_1, u_2, \upsilon_1, \upsilon_2$ for the adherends 1 and 2 one can determine stresses in the adhesive and the adherends. It can be shown [18, 19, 20], that the adhesive stresses are given by

$$\tau_x = \frac{\cos\varphi_x}{1-\sin^2\varphi_x \sin^2\varphi_y}\cdot n_x - \frac{\sin\varphi_x \sin\varphi_y \cos\varphi_y}{1-\sin^2\varphi_x \sin^2\varphi_y}\cdot n_y, \tag{10.a}$$

$$\tau_y = -\frac{\sin\varphi_x \sin\varphi_y \cos\varphi_x}{1-\sin^2\varphi_x \sin^2\varphi_y}\cdot n_x + \frac{\cos\varphi_y}{1-\sin^2\varphi_x \sin^2\varphi_y}\cdot n_y, \tag{10.b}$$

$$\sigma_N = \left(\tau_x \sin\varphi_x + \tau_y \sin\varphi_y\right)\sqrt{1+\mathrm{tg}^2\varphi_x + \mathrm{tg}^2\varphi_y}\,, \tag{10.c}$$

where:

$$n_x = \frac{G_s}{t}\left[\delta_u(u_1-u_2) + \delta_{u\upsilon}(\upsilon_1-\upsilon_2)\right], \tag{11.a}$$

$$n_y = \frac{G_s}{t}\left[\delta_{\upsilon u}(u_1-u_2) + \delta_{\upsilon}(\upsilon_1-\upsilon_2)\right]. \tag{11.b}$$

Stresses in the adherends made from an orthotropic material are expressed by:

$$\sigma_{kx} = \frac{E_{kx}}{1-\nu_{kxy}\nu_{kyx}}\cdot\frac{\partial u_k}{\partial x} + \frac{\nu_{kxy}E_{kx}}{1-\nu_{kxy}\nu_{kyx}}\cdot\frac{\partial \upsilon_k}{\partial y}, \tag{12.a}$$

$$\sigma_{ky} = \frac{\nu_{kyx}E_{ky}}{1-\nu_{kxy}\nu_{kyx}}\cdot\frac{\partial u_k}{\partial x} + \frac{E_{ky}}{1-\nu_{kxy}\nu_{kyx}}\cdot\frac{\partial \upsilon_k}{\partial y}, \tag{12.b}$$

$$\tau_{kxy} = G_{kxy}\left(\frac{\partial u_k}{\partial y} + \frac{\partial \upsilon_k}{\partial x}\right), \tag{12.c}$$

where $k = 1$ for the adherend 1 and $k = 2$ for the adherend 2.

4. STRESS EQUATIONS FOR ADHESIVE

In the particular case, when the adherends are plane, of a constant thickness and made from orthotropic materials, the displacement equations (1.a) – (1.d) can be transformed to the form where shear stresses in the adhesive are unknowns. This yields [18, 19, 21]:

$$(1+\alpha)\frac{\partial^2 \tau_x}{\partial x^2} + \frac{\partial^2 \tau_x}{\partial y^2} + \alpha\frac{\partial^2 \tau_y}{\partial x \partial y} - k^2\tau_x + \frac{G_s}{t}\left(\frac{q_{1x}}{g_1 G_1} - \frac{q_{2x}}{g_2 G_2}\right) = 0, \tag{13.a}$$

$$\frac{\partial^2 \tau_y}{\partial x^2} + (1+\alpha)\frac{\partial^2 \tau_y}{\partial y^2} + \alpha\frac{\partial^2 \tau_x}{\partial x \partial y} - k^2\tau_y + \frac{G_s}{t}\left(\frac{q_{1y}}{g_1 G_1} - \frac{q_{2y}}{g_2 G_2}\right) = 0, \tag{13.b}$$

where

$$\alpha = \frac{1+\nu}{1-\nu}, \tag{14}$$

$$\nu = 0{,}5(\nu_1 + \nu_2), \tag{15}$$

$$k^2 = \frac{G_s}{t}\left(\frac{1}{g_1 G_1} + \frac{1}{g_2 G_2}\right) = \frac{2(1+\nu)G_s}{t}\left(\frac{1}{g_1 E_1} + \frac{1}{g_2 E_2}\right), \tag{16}$$

and ν_1 , ν_2 are Poisson's ratios for the adherends 1 and 2.
Static boundary conditions for the shear stresses τ_x and τ_y take the form

$$\left(\frac{\partial \tau_x}{\partial x} + \nu\frac{\partial \tau_y}{\partial y}\right)\cdot l + \frac{1-\nu}{2}\left(\frac{\partial \tau_x}{\partial y} + \frac{\partial \tau_y}{\partial x}\right)\cdot m = \frac{(1-\nu^2)G_s}{t}\left(\frac{p_{1x}}{E_1} - \frac{p_{2x}}{E_2}\right), \tag{17.a}$$

$$\frac{1-\nu}{2}\left(\frac{\partial \tau_x}{\partial y} + \frac{\partial \tau_y}{\partial x}\right)\cdot l + \left(\nu\frac{\partial \tau_x}{\partial x} + \frac{\partial \tau_y}{\partial y}\right)\cdot m = \frac{(1-\nu^2)G_s}{t}\left(\frac{p_{1y}}{E_1} - \frac{p_{2y}}{E_2}\right). \tag{17.b}$$

The static boundary conditions (17.a) and (17.b) suffice to ensure uniqueness of solutions to the equations (13.a) and (13.b). It is assumed, that an adhesive joint

is loaded by a self-equilibrated set of external forces, so the shear stresses τ_x and τ_y in the adhesive do not depend on the position of the joint in the space 0XYZ. Thus, for the stress equations kinematic boundary conditions are not formulated. This fact and the stress equations (13.a), (13.b) will be used to verify the solution smoothing method applied to solutions of the displacement equations (1.a) – (1.d) by means of the Dirichlet boundary value problem.

5. NUMERICAL SOLUTION BY THE FINITE DIFFERENCE METHOD

Boundary value problems in displacements and in stresses are solved here, using the classical finite difference method [1, 3, 4, 6, 8, 12, 23]. The method is based on a replacement of differential operators with difference operators defined in a discrete set of points (nodes), which are intersections of lines forming a difference mesh in a rectangle $2l_x \times 2l_y$ (Fig. 2).

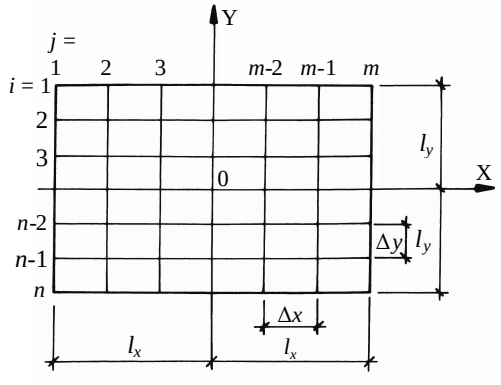

Fig. 2. Finite difference mesh on a projection of adhesive surface

The difference mesh has a regular rectangular shape with side lengths Δx and Δy. There are m nodes in the direction X ($j = 1, 2, ..., m$), and n nodes in the direction Y ($i = 1, 2, ..., n$), with $n, m \geq 5$. It is assumed that n and m are odd numbers. The unknowns in the finite difference method are the values of displacements functions $u_{kr,s} = u_k(x_r, y_s)$ and $v_{kr,s} = v_k(x_r, y_s)$ for $k = 1, 2$ or the values of the shear stresses functions $\tau_{xr,s} = \tau_x(x_r, y_s)$ and $\tau_{yr,s} = \tau_y(x_r, y_s)$ in the adhesive defined in the nodes of the finite difference mesh. Derivatives of functions are approximated with central differences.

Displacement equations are formulated for all the nodes of the finite difference mesh, excluding those, where kinematic boundary conditions are defined and those at sharp edges. In the case of nodes with prescribed kinematic boundary conditions, if they are constrained, zero displacements are substituted. For

nodes on sharp edges static boundary conditions are applied. Application of the central differences to nodes at edges, with the exception of sharp ones, results in fictitious values of unknown functions for nodes falling out of the rectangular domain $2l_x \times 2l_y$. Those fictitious values of the unknown functions are eliminated by means of static boundary conditions for unsharp edges. In the case of sharp edges the fictitious nodes beyond the rectangular domain $2l_x \times 2l_y$ are not introduced. For internal nodes at sharp edges central differences are used for the direction along the edge, while for the direction across edges and for corner nodes unilateral differences spanning three nodes in the direction X and Y are used. A complete set of linear equations of the finite difference method in terms of displacements consists of $4nm$ equations. The matrix formed from coefficients of equations is not symmetric and is singular because the adhesive joint itself is a mechanism. Non-singularity of the matrix and uniqueness of the solution for a system expressed in terms of displacements is obtained, if kinematic boundary conditions for displacements u_k and v_k are imposed to make the adhesive joint geometrically stable. To this end one has to constrain at least three degrees of freedom at arbitrary points of the finite difference mesh at one of the adherends. The constrains can be one- or two-directional. The points and directions subjected to the constraints do not belong to the definition set of the equations but to the boundary points set. Finite difference equations are not formulated for the constrained directions at the boundary points. The described process of imposing of kinematic conditions can be illustrated by an example of a difference mesh $n = m = 5$ presented in Fig. 3. In the analyzed case it is assumed that the point 7 in the adherend 2 has imposed constraints in both directions and the point 14 in the direction Y. Points of the adherend 1 are not constrained.

The kinematic boundary conditions presented in Fig. 3 can be given analytically as:

$$u_2(7) = 0, \quad v_2(7) = 0, \quad v_2(14) = 0 .$$

The stress equations are formulated for all the nodes of the finite difference mesh. In the equations related to the nodes located at boundaries of the rectangle, fictitious values of unknowns at the points lying beyond the rectangular domain $2l_x \times 2l_y$ are present. They are eliminated from the set of equations by means of static boundary conditions.

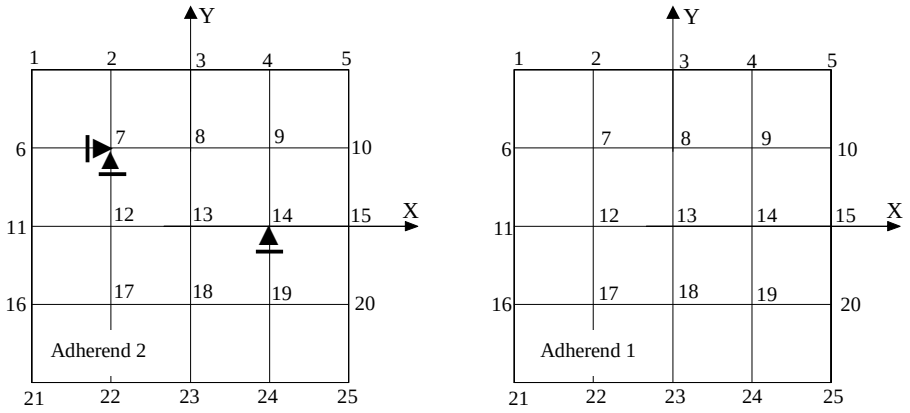

Fig. 3. Example of kinematic boundary conditions
for the finite difference mesh $n = m = 5$

Adherends displacements and stresses as well as shear stresses in adhesive depend on loading and constraining of the adherends. A particular case is represented by an adhesive joint, where one adherend is constrained as statically determinate and the joint is loaded by a self-equilibrated set of forces. Then support reactions at the constraints are zero, independently of the way of constraining. Thus, in such cases adherends displacements depend only on loading and layout of constraints, while stresses in adherends and adhesive – on loading only.

Numerical solutions to displacements and stress based boundary value problems discussed above were obtained using a system of computer programs SPOINA (ADHESIVE). For elliptic equations of the theory of elasticity the finite difference method is convergent [2, 16]. Test computations indicate, that the finite difference meshes from the range $41 \leq m, n \leq 51$ yield a relative error of solution not exceeding 0.5%.

6. NUMERICAL NON-EQUILIBRIUM

In the case of displacement formulation solutions are sensitive to kinematic boundary conditions. It can be observed for adhesive joints with one adherend constrained to be statically determinate (like in Fig. 3) and a self-equilibrated loading set. In this case support reactions should be zero. However, the solutions to the displacement based finite difference equations usually do not fulfil this condition. The solutions feature numerical errors and the joint

behaves as if it was not in equilibrium. Here this phenomenon is called *numerical non-equilibrium*.

The numerical non-equilibrium is manifested in disturbances of solutions in the form of small global asymmetry and local concentrations at constrained points of the finite difference mesh.

The numerical error consists of a method error and round-up errors. The method error is due to the discretisation of the adhesive joint domain by the finite difference mesh and replacement of derivatives in the equations with finite differences.

The round-up errors occur during arithmetic computation and their magnitude depends on the type of operation and machine precision, i.e. the number of bits used to store the real number in computer memory (32 bits in single precision, 64 bits in double precision and 80 in extended precision). In the examples presented in this paper the method error does not influence the form and magnitude of the numerical non-equilibrium. The precision of computations plays a vital role here.

In order to illustrate the phenomenon of the numerical non-equilibrium an adhesive joint loaded axially is analyzed. The joint consists of two steel adherends with the following dimensions: length 10.0 cm (l_x = 5.0 cm), width 8.0 cm (l_y = 4.0 cm). The adherend thickness is $g_1 = g_2$ = 0.4 cm, and the adhesive thickness is t = 0.04 cm. The adopted modulus of deformability for adhesive is G_s = 450000 N/cm^2 and the difference mesh $n \times m = 41 \times 51$ ($\Delta x = \Delta y$ = 0.2 cm). The edges $x = l_x$ of the adherend 1 and $x = -l_x$ of the adherend 2 are subjected to a uniformly distributed normal loading $\pm\sigma$ = 2.5 N/cm^2. The loading resultants acting at the adherend edges are $\mathsf{N}_{1p} = -\mathsf{N}_{2L}$ = 8.0 N. Kinematic boundary conditions are imposed on the adherend 2 to constrain the point (21, 26) in the directions X, Y and the point (21, 36) in the direction Y, see Fig. 4.

A complete solution to the problem in the displacement formulation is given as functions of adherends displacements u_k , v_k , functions of stresses in adherends σ_{kx} , σ_{ky} , τ_{kxy} , (k = 1, 2) and functions of shear stresses in adhesive τ_x and τ_y. First, solutions obtained using single precision are analyzed. Figures 6*a*, *b* – 7.13*a*, *b* present distributions of functions u_k , v_k , σ_{kx} , σ_{ky} , τ_{kxy} , τ_x and τ_y with an

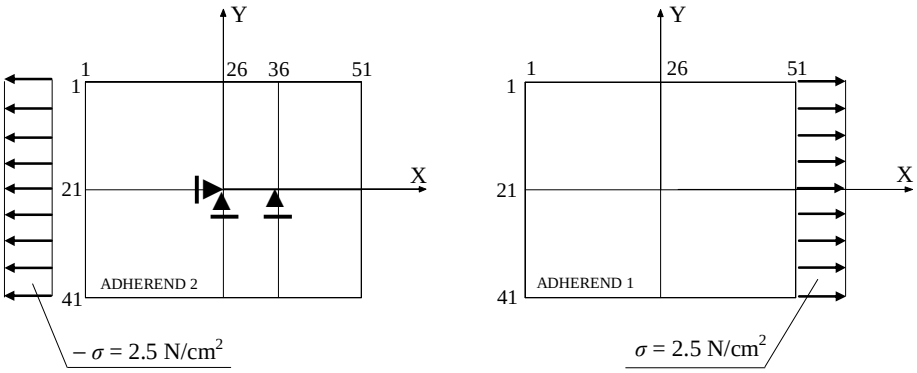

Fig. 4. Loading and constraining of adherends in an adhesive joint

indication of boundary disturbances to displacements and stresses due to constraining of the adherend 2. These disturbances can be decreased or eliminated by a correction of loading acting on the joint. There are many ways to correct the loading but any correction will violate the equilibrium of the original loading system. It was found by a trial-and-error approach, that the disturbances in stresses and displacements distributions can be decreased by a correction of the loading acting on the adherend l with the forces $N_{1g} = N_{1d} = -0.0015$ N, $N_{1L} = N_{1p} = -0.001725$ N and $T_{1p} = -0.000091$ N. These forces in the form of uniformly distributed stresses along edges of the adherend 1 are presented in Fig. 5. Effects of this decrease of disturbances in the distributions of displacements and stresses are shown in Figs. 6*c* – 11*c*.

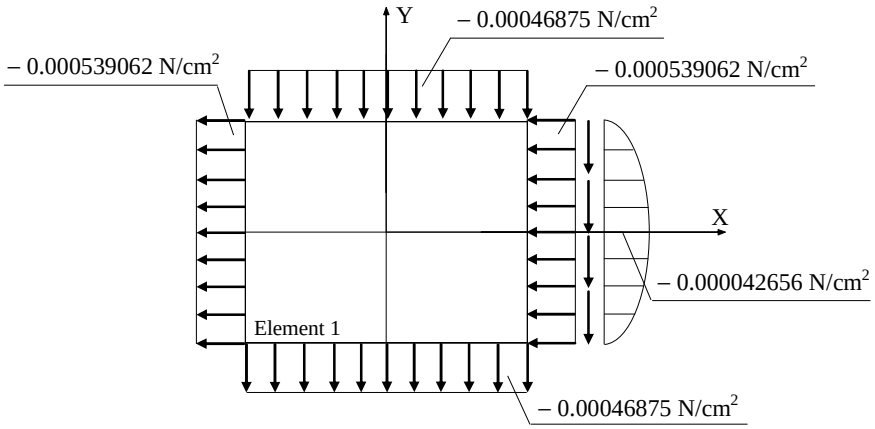

Fig. 5. Correction of loading acting on adherend 1

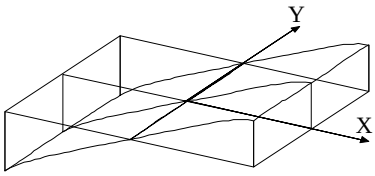

Displacement u_2 in adherend 2

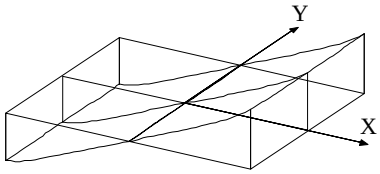

Displacement u_1 in adherend 1

a) Distributions of displacements functions u_1 and u_2

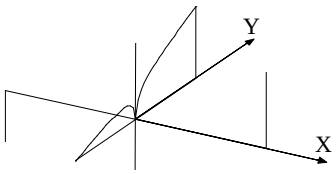

Displacement u_2 in adherend 2

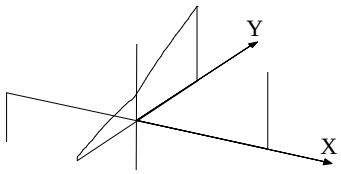

Displacement u_1 in adherend 1

b) Disturbances in distributions of displacements u_1 and u_2 along Y. 500-times magnification

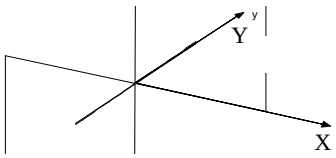

placement u_2 in adherend 2

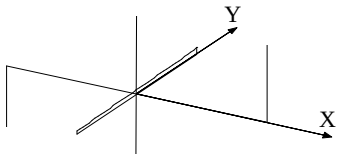

Displacement u_1 in adherend 1

c) Decrease of disturbances in distributions of displacements u_1 and u_2 due to correction of adherend 1 loading presented in Fig. 5. 500-times magnification

Fig. 6. Illustration of numerical non-equilibrium for displacements u_1 and u_2 in steel-steel adhesive joint loaded axially and constrained according to Fig. 4. Single precision computations

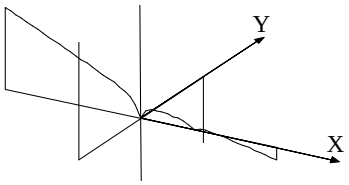

Displacement v_2 in adherend 2

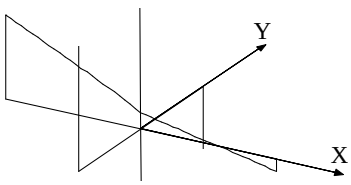

Displacement v_1 in adherend 1

b) Disturbances in distributions of displacements v_1 and v_2 along Y. 500-times magnification

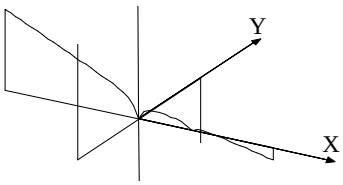

Displacement v_2 in adherend 2

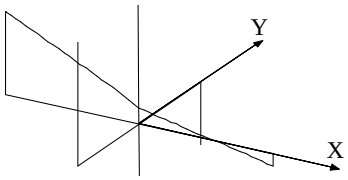

Displacement v_1 in adherend 1

b) Disturbances in distributions of displacements v_1 and v_2 along Y. 500-times magnification

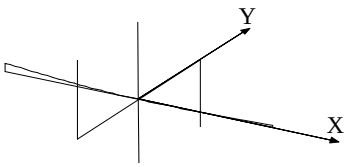

Displacement v_2 in adherend 2

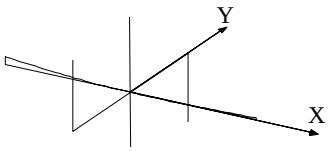

Displacement v_1 in adherend 1

c) Decrease of disturbances in distributions of displacements v_1 and v_2 due to correction of adherend 1 loading presented in Fig. 5. 500-times magnification

Fig. 7. Illustration of numerical non-equilibrium for displacements v_1 and v_2 in steel-steel adhesive joint loaded axially and constrained according to Fig. 4. Single precision computations

The values of displacements u_1 and u_2 at the axis X in Fig.6*a* are:

$u_1(-l_x,0) = -2.6874\cdot10^{-7}$cm, $u_1(0,0) = 3.0407\cdot10^{-10}$cm, $u_1(l_x,0) = 3.3931\cdot10^{-7}$cm,

$u_2(-l_x,0) = -3.3846\cdot10^{-7}$cm, $u_2(0,0) = 0.0$cm, $u_2(l_x,0) = 2.6948\cdot10^{-7}$cm.

The values of displacements v_1 and v_2 at the axis Y in Fig.7*a* are:

$$v_1(0,-l_y) = 6{,}8327\cdot10^{-8}\text{cm},\ v_1(0,0) = 1{,}7424\cdot10^{-10}\text{cm},\ v_1(0,l_y) = -6{,}7824\cdot10^{-10}\text{cm},$$

$$v_2(0,-l_y) = 6{,}8312\cdot10^{-8}\text{cm},\ v_2(0,0) = 0{,}0\,\text{cm},\ v_2(0,l_y) = -6{,}7808\cdot10^{-10}\text{cm}.$$

Figure 6*b* presents a constraint at the point $(i, j) = (21, 26)$ of the adherend 2 in the direction X, and Fig. 7*b* – a constraint of the adherend 2 at the points $(i, j) = (21, 26)$ and $(i, j) = (21, 36)$ in the direction Y, according to the kinematic boundary conditions imposed on the adherend 2 (Fig. 4). Local concentrations of displacements distributions were formed at the constrained points. Figures depict certain asymmetry of displacements along axes X an Y, too.
By means of an appropriate correction the concentration and asymmetry can be decreased (Figs. 6*c* and 7*c*).

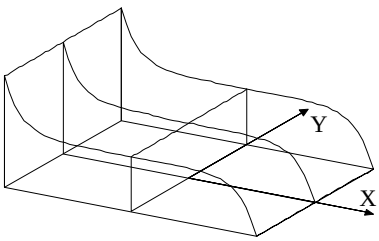

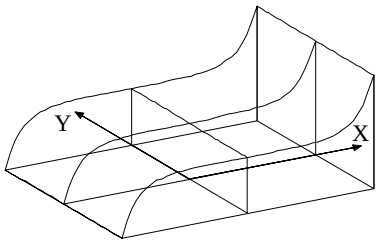

Normal stress σ_{2x} in adherend 2 Normal stress σ_{1x} in adherend 1

a) Distributions of normal stresses functions σ_{1x} , σ_{2x} in adherends

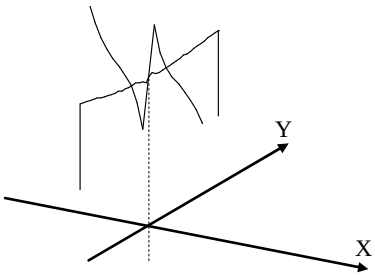

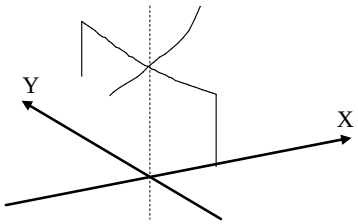

Normal stress σ_{2x} in adherend 2 Normal stress σ_{1x} in adherend 1

b) Disturbances in distributions of normal stresses σ_{1x} , σ_{2x}. 100-times magnification

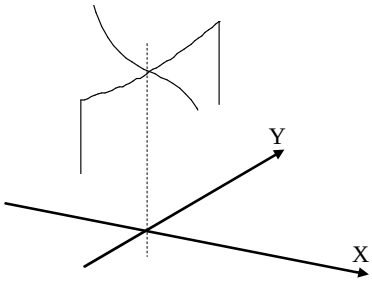

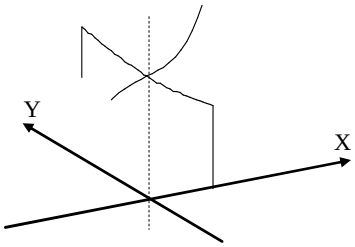

Normal stress σ_{2x} in adherend 2 Normal stress σ_{1x} in adherend 1

c) Eliminated disturbances in distributions of normal stresses σ_{1x} , σ_{2x} due to correction of adherend 1 loading presented in Fig. 5. 100-times magnification

Fig. 8. Illustration of numerical non-equilibrium for stresses σ_{1x} , σ_{2x} in steel-steel adhesive joint loaded axially and constrained according to Fig. 4. Single precision computations

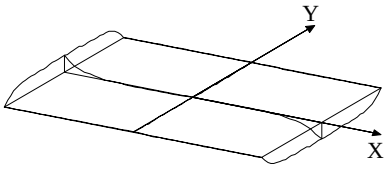

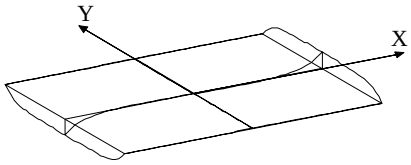

Normal stress σ_{2y} in adherend 2 Normal stress σ_{1y} in adherend 1

a) Distributions of normal stresses functions σ_{1y} , σ_{2y} in adherends

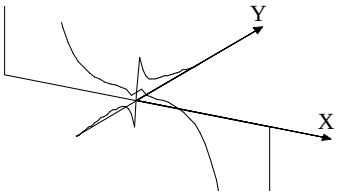

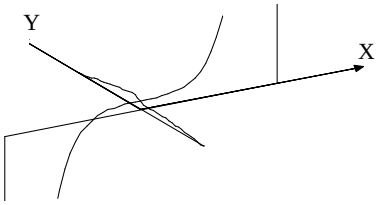

Normal stress σ_{2y} in adherend 2 Normal stress σ_{1y} in adherend 1

b) Disturbances in distributions of normal stresses σ_{1y} , σ_{2y}. 100-times magnification

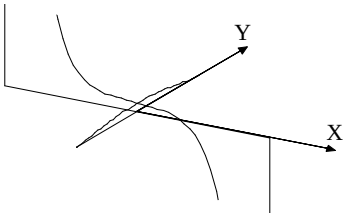

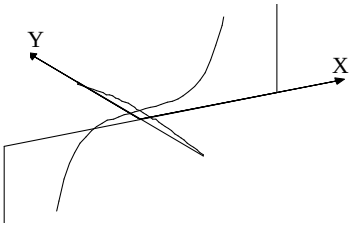

Normal stress σ_{2y} in adherend 2 Normal stress σ_{1y} in adherend 1

c) Eliminated disturbances in distributions of normal stresses σ_{1y} , σ_{2y} due to correction of adherend 1 loading presented in Fig. 5. 100-times magnification

Fig. 9. Illustration of numerical non-equilibrium for stresses σ_{1y} , σ_{2y} in steel-steel adhesive joint loaded axially and constrained according to Fig. 4. Single precision computations

The stress values σ_{1x} , σ_{1y} at the axis X in Fig. 8*a* i 9*a* are:

$$\sigma_{1x}(-l_x,0) = 0{,}0\ \mathrm{N/cm^2},\ \sigma_{1x}(0,0) = 1{,}25\ \mathrm{N/cm^2},\ \sigma_{1x}(l_x,0) = 2{,}5\ \mathrm{N/cm^2},$$
$$\sigma_{1y}(-l_x,0) = -0{,}35\ \mathrm{N/cm^2},\ \sigma_{1y}(0,0) = 0{,}0\ \mathrm{N/cm^2},\ \sigma_{1y}(l_x,0) = 0{,}35\ \mathrm{N/cm^2}.$$

The shear stresses τ_{1xy}, τ_{2xy} in the adherends are antisymmetric.

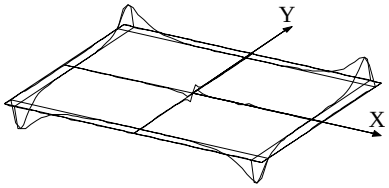

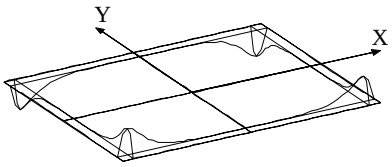

Shear stress τ_{2xy} in adherend 2 Shear stress τ_{1xy} in adherend 1

a) Distributions of shear stresses functions τ_{1xy} , τ_{2xy} in adherends

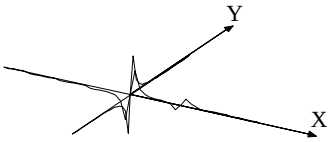

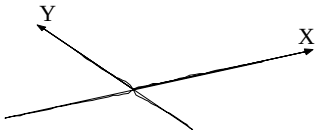

Shear stress τ_{2xy} in adherend 2 Shear stress τ_{1xy} in adherend 1

b) Disturbances in distributions of shear stresses τ_{1xy} , τ_{2xy}. 5-times magnification

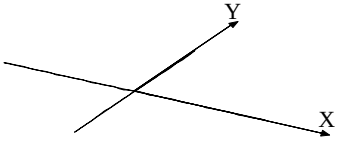

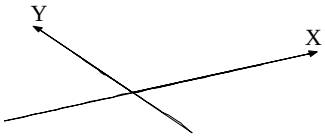

Shear stress τ_{2xy} in adherend 2 Shear stress τ_{1xy} in adherend 1

c) Eliminated disturbances in distributions of shear stresses τ_{1xy} , τ_{2xy} due to the correction of adherend 1 loading presented in Fig. 5. 5-times magnification

Fig. 10. Illustration of numerical non-equilibrium for shear stresses τ_{1xy} , τ_{2xy} adherends of steel-steel adhesive joint loaded axially and constrained according to Fig. 4. Single precision computations

The extreme value of τ_{kxy} in the adherends in Fig. 10*a* is $\tau_{kxy} = \pm 0{,}0148 \mathrm{N/cm}^2$.

It can be concluded from Figs. 6*b* – 12*b* that the disturbances of displacements and stresses in the adherend 2, due to its constraining, are transmitted to an insignificant degree to the adherend 1 – they are moderated in adhesive due to its flexibility. However, this moderation results in local concentrations of shear stress in adhesive, presented in Fig. 11*b*.

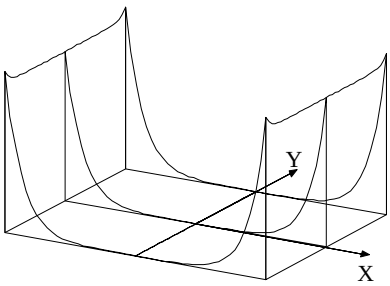

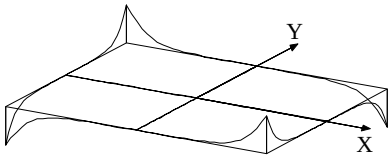

Shear stress τ_x in adhesive Shear stress τ_y in adhesive

a) Distributions of shear stresses functions in adhesive: $\tau_x(\pm l_x , 0) = 0.785$ N/cm^2, $|\tau_y(\pm l_x , \pm l_y)| = 0.199$ N/cm^2

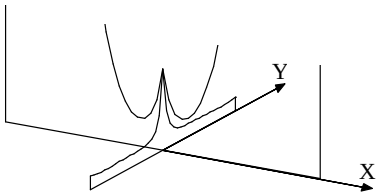

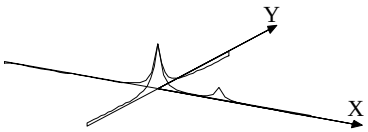

Shear stress τ_x in adhesive Shear stress τ_y in adhesive

b) Concentrations of shear stresses in adhesive. 100-times magnification

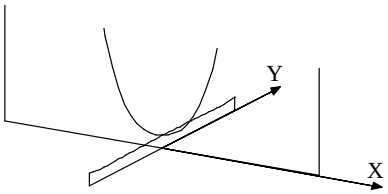

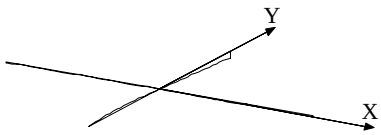

Shear stress τ_x in adhesive Shear stress τ_y in adhesive

c) Shear stresses in adhesive after elimination of concentrations due to correction of adherend 1 loading presented in Fig. 5. 100-times magnification

Fig. 11. Illustration of numerical non-equilibrium for shear stresses in adhesive of steel-steel adhesive joint loaded axially and constrained according to Fig. 4. Single precision computations

Numerical errors in the case of extended precision are much smaller than for single precision and computations do not require any corrections. For instance, the displacements u_1 and u_2 along the axes X and Y presented with a magnitude possible to represent in figures are symmetric, regular and do not exhibit any disturbances in the form of local concentrations at the constrained points of the

adherend 2 (Fig. 12*a*, *b*). The displacements v_1 and v_2 , which should be zero at the axis X, do not exhibit any local disturbances even for 10^{13} -times magnification and in the scale used in figures can be considered as null (Fig. 12*c*).

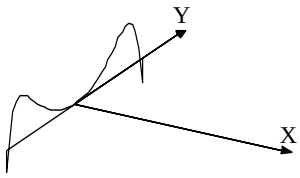

a) Displacement u_2 in adherend 2 at the axis Y. 10^5-times magnification with respect to Fig. 6a

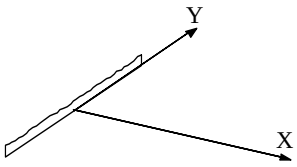

b) Displacement u_1 in adherend 1 at the axis Y. 10^3-times magnification with respect to Fig. 6a

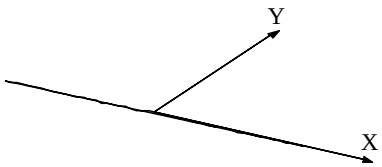

c) Displacements v_1 and v_2 at the axis X. 10^{13}-times magnification with respect to Fig. 7a

Fig. 12. Absence of any evident disturbances of displacements in steel-steel adhesive joint loaded axially and constrained according to Fig. 4. Extended precision computations

Distributions of stresses τ_x and τ_y do not exhibit any concentrations at the constrained points for the adherend 2 even at 100-times magnification (Fig. 13*a*). Larger magnification does not indicate any concentrations for the stress τ_x, while some concentrations of τ_y become evident for 10^{14}-times magnification. Also the signs of stress values τ_y are different at the concentrations (Fig. 13*b*).

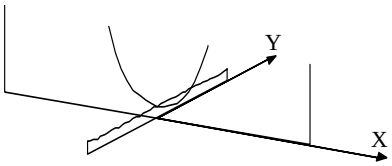

Shear stress τ_x in adhesive

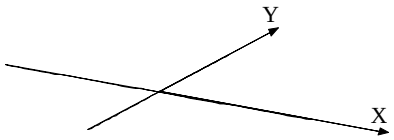

Shear stress τ_y in adhesive

a) Distributions of shear stresses functions in adhesive along the axes X, Y. 100-times magnification with

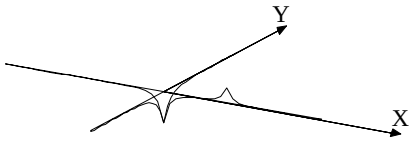

b) Concentrations of shear stresses τ_y in adhesive at the constrained points in the adherend 2. 10^{14}-times magnification with respect to Fig. 11a

Fig. 13. Illustration of numerical non-equilibrium in adhesive of steel-steel adhesive joint loaded axially and constrained according to Fig. 4. Extended precision computations

7. SOLUTIONS SMOOTHING

The presented method to remove local disturbances of displacements and stresses based on a correction of loading acting on an adhesive joint was meant to illustrate the numerical non-equilibrium only. It is not appropriate for practical purposes because it involves numerous repetitions of the computations and is not unique. A more correct method to improve the situation is *solution smoothing*.

This method is based on the observation (founded, for instance, by Figs. 6–13 and numerical results), that an influence of local disturbances of displacements is limited to a small zone on the joint surface around a constrained point. Thus, if the constrained point were located at a sufficient distance from the adhesive edges, than local disturbances at that point would have a negligible influence on solutions at points lying at the edges of the adhesive surface.

The proposed method of solution smoothing involves two subsequent solutions of different boundary value problems for one adhesive joint. In the first problem, solution to the equations (1.a) – (1.d) fulfilling the static boundary conditions (5.a) – (5.d) or (6.a) – (6.d) and kinematic boundary conditions is found. The static boundary conditions include loading acting on the adhesive joint and the kinematic boundary conditions – constraining of one of adherends ensuring geometric stability of the adhesive joint.

Having solved the first problem one gets the functions of displacements of adherends defined at the entire adhesive surface. Thus, the functions of displacements at the adhesive edges are known, too. If the constrained points are sufficiently remote from the adhesive edges, then one can assume, that the functions of displacements at the adhesive edges do not exhibit errors due to local displacement concentrations. These functions as given continuous functions in the definition domain for the equations (1.a) – (1.d), can be treated

as boundary functions for the second boundary value problem, namely the *Dirichlet boundary problem* [11, 14, 17].

To formulate the Dirichlet boundary problem the notation $\overline{\Omega}$ is introduced for a closed rectangle coinciding with a projection of an adhesive surface on the plane 0XY of the main set of co-ordinates and it is defined as a Cartesian product of two closed sections $[-l_x, l_x] \subset \mathsf{R}$ and $[-l_y, l_y] \subset \mathsf{R}$, i.e.

$$\overline{\Omega} = [-l_x, l_x] \times [-l_y, l_y].$$

The interior of $\overline{\Omega}$ is an open rectangle Ω defined as a Cartesian product of two open sections $(-l_x, l_x) \subset \mathsf{R}$ and $(-l_y, l_y) \subset \mathsf{R}$, i.e.

$$\Omega = (-l_x, l_x) \times (-l_y, l_y).$$

The set Ω on the plane R^2, as connected and open, represents a region in R^2. The boundary $\partial\Omega$ of the region Ω is defined as a difference of sets $\partial\Omega = \overline{\Omega} \setminus \Omega$. The sets $\partial\Omega$ and Ω are disjoint and the equality $\overline{\Omega} = \Omega \cup \partial\Omega$ holds. On the boundary $\partial\Omega$ of the region Ω, i.e. for $(x, y) \in \partial\Omega$, continuous functions

$$u_{1b}(x, y), \quad \upsilon_{1b}(x, y), \quad u_{2b}(x, y), \quad \upsilon_{2b}(x, y) \tag{18}$$

are given. They define displacements of adherends at the adhesive surface.

The Dirichlet problem (the internal Dirichlet boundary value problem) for the equations (1.a) – (1.d) requires finding the functions $u_1, \upsilon_1, u_2, \upsilon_2$, defined and continuous in the set $\overline{\Omega}$, having continuous second partial derivatives defined in the region Ω, fulfilling the equations (1.a) – (1.d) in Ω, and fulfilling the Dirichlet boundary conditions:

$$u_1(x, y)\big|_{\partial\Omega} = u_{1b}(x, y), \tag{19.a}$$

$$\upsilon_1(x, y)\big|_{\partial\Omega} = \upsilon_{1b}(x, y), \tag{19.b}$$

$$u_2(x, y)\big|_{\partial\Omega} = u_{2b}(x, y), \tag{19.c}$$

$$\upsilon_2(x, y)\big|_{\partial\Omega} = \upsilon_{2b}(x, y) \tag{19.d}$$

at the boundary of the region Ω, i.e. for $(x, y) \in \partial\Omega$. The boundary conditions (18) have the sense of limit transformations from the interior of the region Ω onto its boundary $\partial\Omega$. It means, that for an arbitrary point $(x_b, y_b) \in \partial\Omega$ and for $(x, y) \in \Omega$ the following limits exist:

$$\lim_{(x,y)\to(x_b,y_b)} u_1(x,y) = u_{1b}(x_b, y_b),$$
$$\lim_{(x,y)\to(x_b,y_b)} \upsilon_1(x,y) = \upsilon_{1b}(x_b, y_b),$$
$$\lim_{(x,y)\to(x_b,y_b)} u_2(x,y) = u_{2b}(x_b, y_b),$$
$$\lim_{(x,y)\to(x_b,y_b)} \upsilon_2(x,y) = \upsilon_{2b}(x_b, y_b).$$

Thus, we have defined uniquely the solutions to two following boundary value problems:

– to the boundary problem (1.a) – (1.d), (6.a) – (6.d) or (7.a) – (7.d) in displacements with kinematic boundary conditions denoted by $u_{1S}, \upsilon_{1S}, u_{2S}, \upsilon_{2S}$,

– to the Dirichlet boundary problem denoted by $u_{1D}, \upsilon_{1D}, u_{2D}, \upsilon_{2D}$.

These solutions are identical. In order to prove it, it is sufficient to note, that the functions given by:

$$\Delta u_1 = u_{1S} - u_{1D}, \quad \Delta\upsilon_1 = \upsilon_{1S} - \upsilon_{1D}, \quad \Delta u_2 = u_{2S} - u_{2D}, \quad \Delta\upsilon_2 = \upsilon_{2S} - \upsilon_{2D}$$

fulfil the equations (7.a) with zero Dirichlet boundary conditions:

$$\Delta u_1(x,y)\big|_{\partial\Omega} = 0, \quad \Delta\upsilon_1(x,y)\big|_{\partial\Omega} = 0, \quad \Delta u_2(x,y)\big|_{\partial\Omega} = 0, \quad \Delta\upsilon_2(x,y)\big|_{\partial\Omega} = 0. \tag{20}$$

Uniqueness of the solution to the Dirichlet boundary problem leads to zero solutions for zero boundary conditions. Hence,

$$\Delta u_1 = 0, \quad \Delta\upsilon_1 = 0, \quad \Delta u_2 = 0, \quad \Delta\upsilon_2 = 0, \tag{21}$$

yielding $(u_{1S}, \upsilon_{1S}, u_{2S}, \upsilon_{2S}) = (u_{1D}, \upsilon_{1D}, u_{2D}, \upsilon_{2D})$.

The identity of these solutions has purely theoretical meaning. The numerical solutions u_{1S}, υ_{1S}, u_{2S}, υ_{2S} and u_{1D}, υ_{1D}, u_{2D}, υ_{2D} are not identical in reality. The solutions u_{1S}, υ_{1S}, u_{2S}, υ_{2S} feature disturbances in the form of local concentrations at the constraining points, while the solutions u_{1D}, υ_{1D}, u_{2D}, υ_{2D} are free of them because the Dirichlet boundary value problem involves the

displacement functions for adherends, which, in the region Ω, fulfil the equations (1.a) – (1.d) exclusively, without any additional conditions.
Thus, the numerical solutions u_{1D} , v_{1D} , u_{2D}, v_{2D} of the Dirichlet boundary value problem are the smooothed solutions of the problem with static and kinematic boundary conditions
Hence, for the Dirichlet boundary value problem the region Ω is the set of definition of the equations (1.a) – (1.d). The finite difference equations are formulated for internal nodes of a finite difference mesh only, while for edge nodes values of displacements of adherends at an adhesive edge computed in the first boundary value problem are substituted.
Effects of smoothing of concentrations in the solution shown in Figs. 6–11, using the solutions to the Dirichlet boundary value problem, are presented in Figs. 14–16.

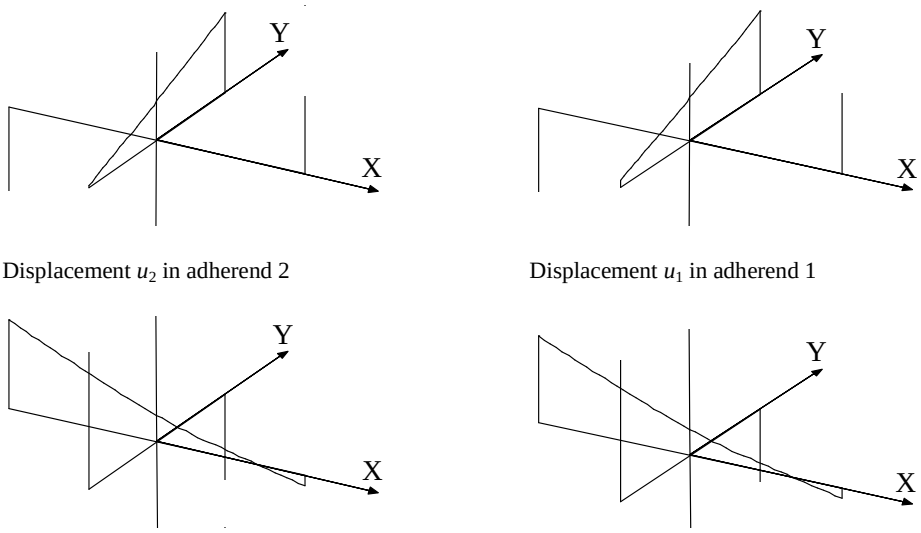

Displacement u_2 in adherend 2 | Displacement u_1 in adherend 1

Displacement v_2 in adherend 2 | Displacement v_1 in adherend 1

Fig. 14. Smoothing of local concentrations in displacements u_1, u_2, v_1 and v_2 shown in Figs. 6*b* and 7*b* using solution to the Dirichlet boundary value problem. 500-times magnification with respect to Figs. 6*a* and 7*a*. Single precision computations

Accuracy of a solution to the finite difference problem formulated in displacements can be assessed indirectly by a comparison to a solution considered as exact. One may assume, that the exact solution is given as the functions of shear stresses in adhesive τ_x and τ_y obtained from the boundary value problem expressed in stresses (13.a) – (13.b), (17.a) – (17.b).

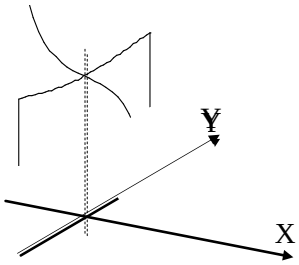

Normal stress σ_{2x} in adherend 2

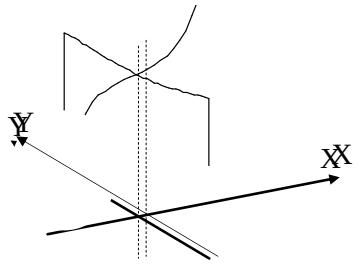

Normal stress σ_{1x} in adherend 1

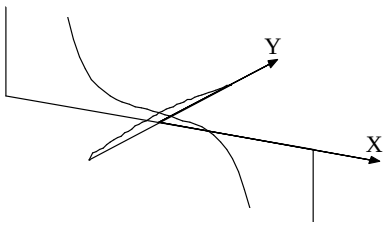

Normal stress σ_{2y} in adherend 2

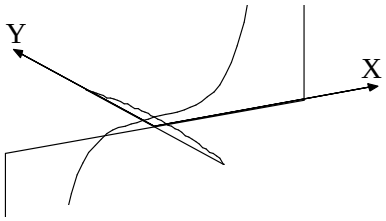

Normal stress σ_{1y} in adherend 1

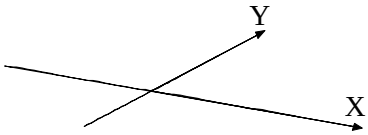

Shear stress τ_{2xy} in adherend 2

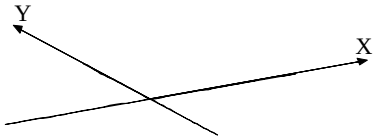

Shear stress τ_{1xy} in adherend 1

Fig. 15. Smoothing of local concentrations in stresses σ_{kx} , σ_{ky} , τ_{kxy} shown in Figs. 8*b* – 10*b* using solution to the Dirichlet boundary value problem. 100-times magnification with respect to Figs. 8*a* – 10*a*. Single precision computations

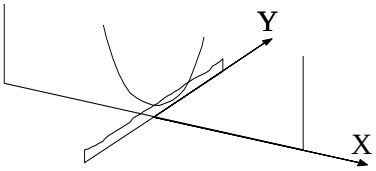

Shear stress τ_x in adhesive

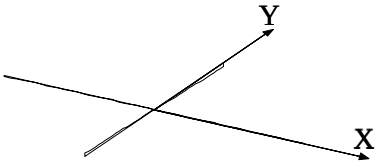

Shear stress τ_y in adhesive

Fig. 16. Smoothing of local concentrations in stresses τ_x and τ_y shown in Fig. 11*b* using solution to the Dirichlet boundary value problem. 100-times magnification with respect to Fig. 11*a*. Single precision computations

Such an assumption is justified because stress formulations do not involve any kinematic boundary conditions and the phenomenon of numerical non-equilibrium does not occur.

Besides, there are two times fewer difference equations than in the displacement formulation. Thus, solutions for a stress problem features a smaller numerical error.

Values of the shear stresses τ_x and τ_y in adhesive (in the considered case $\sigma_N = 0$) of the analyzed steel-steel joint loaded axially at arbitrary nodes of the finite difference mesh can be calculated from the formulae (10.a) – (10.b) basing on the solutions to the Dirichlet boundary value problem (a smoothed solution to the problem in displacements) and to the problem formulated in stresses. Some results obtained with single precision computations are given in Tables 1 and 2.

Table 1. Values of shear stresses in adhesive [N/cm^2] at Fig. 11*a* from solution to the Dirichlet boundary value problem, single precision.

*i**j*		1	26	51
1	τ_x	8.486827E-1	5.917435E-4	8.493129E-1
	τ_y	1.992273E-1	– 1.872102E-4	– 1.993071E-1
21	τ_x	7.843243E-1	5.662714E-4	7.855886E-1
	τ_y	– 2.296725E-5	– 1.467888E-6	– 2.127704E-5
41	τ_x	8.486575E-1	5.865992E-4	8.492196E-1
	τ_y	– 1.992173E-1	1.629896E-4	1.993295E-1

Table 2. Values of shear stresses in adhesive [N/cm^2] at Fig. 11*a*, single precision.

*i**j*		1	26	51
1	τ_x	8.489776E-1	5.909367E-4	8.489777E-1
	τ_y	1.992904E-1	2.414237E-10	– 1.992906E-1
21	τ_x	7.850467E-1	5.655336E-4	7.850462E-1
	τ_y	– 8.30481E-8	8.998684E-10	1.059868E-7
41	τ_x	8.489764E-1	5.909268E-4	8.489764E-1
	τ_y	– 1.992903E-1	– 1.293227E-10	1.992905E-1

Errors of the solution to the Dirichlet boundary value problem given in Table 1 with respect to the solution of the problem in stresses given in Table 2 treated as the exact solution are presented in Table 3.

Table 3. Errors in % of solution to the Dirichlet boundary value problem from Table 1 with respect to the solution of the problem in stresses in Table 2, single precision

*i**j*		1	26	51
1	τ_x	– 0.0347	0.1365	0.0395
	τ_y	– 0.0317	–	– 0.0828

21	τ_x	– 0.0920	0.1305	0.0691
	τ_y	–	–	–
41	τ_x	– 0.0376	– 0.7323	0.0286
	τ_y	0.0366	–	0.0196

Zero values in Table 3 (as well as Table 6) were denoted by "–".

Smoothing eliminates disturbances in solutions in the form of local concentrations at internal nodes of the finite difference mesh only. It does not help to eliminate a solution asymmetry, characteristic for single precision computations. That asymmetry has a global character influencing the entire adhesive surface including displacement values adopted for the Dirichlet boundary value problem. Thus, after smoothing of local concentrations, asymmetry remains, what is evident for displacements in Fig. 14 and for stresses in Tables 1 and 3.

A solution to the Dirichlet boundary value problem obtained using extended precision features symmetry of the stress τ_x and antisymmetry of the stress τ_y in adhesive with 13 or 14 digit accuracy (Table 4), while for the problem in stresses – with 15 digits accuracy (Table 5). Equivalence of the solutions (u_{1S} , v_{1S} , u_{2S} , v_{2S}) = (u_{1D} , v_{1D} , u_{2D} , v_{2D}) in the case of extended precision is fulfilled with 8 or 9 digits accuracy (Tables 4 and 5). Errors (in %) of the solutions to the Dirichlet boundary value problem from Table 4 with respect to the solution of the stress problem given in Table 5, are presented in Table 6.

Table 4. Values of shear stresses in adhesive [N/cm^2] at Fig. 11*a* from solution to the Dirichlet boundary value problem in displacements, extended precision

$i\backslash j$		1	26	51
1	τ_x	8.4897784910685E-1	5.9094202580289E-4	8.4897784910685E-1
	τ_y	1.9929163997762E-1	0	– 1.9929163997763E-1
21	τ_x	7.8504803534036E-1	5.6553379686515E-4	7.8504803534036E-1
	τ_y	– 3.988088577E-18	– 3.5925806786625E-19	1.7690792911054E-17
41	τ_x	8.4897784910685E-1	5.9094202580288E-4	8.4897784910685E-1
	τ_y	– 1.9929163997762E-1	0	1.9929163997762E-1

Table 5. Values of shear stresses in adhesive [N/cm^2] at Fig. 11*a*. Solution to the problem in stresses, extended precision

$i\backslash j$		1	26	51
1	τ_x	8.48977849068113E-1	5.90942025558641E-4	8.48977849068113E-1
	τ_y	1.99291639968777E-1	– 6.61275438283593E-23	– 1.99291639968777E-1
21	τ_x	7.85048035298519E-1	5.65533796605446E-4	7.85048035298519E-1
	τ_y	2.65825758479839E-19	2.56760694084481E-23	– 2.02273481244121E-19
41	τ_x	8.48977849068113E-1	5.90942025558641E-4	8.48977849068113E-1

	τ_y	– 1.99291639968777E-1	– 7.51033902896203E-22	1.99291639968777E-1

Table 6. Errors in % of the stresses obtained from the Dirichlet boundary value problem in Table 4 with respect to the solution of the problem in stresses in Table 5, extended precision

$i\backslash j$		1	26	51
1	τ_x	$0.456 \cdot 10^{-8}$	$0.414 \cdot 10^{-7}$	$0.456 \cdot 10^{-8}$
	τ_y	$0.444 \cdot 10^{-8}$	–	$0.444 \cdot 10^{-8}$
21	τ_x	$0.533 \cdot 10^{-8}$	$0.459 \cdot 10^{-7}$	$0.533 \cdot 10^{-8}$
	τ_y	–	–	–
41	τ_x	$0.456 \cdot 10^{-8}$	$0.414 \cdot 10^{-7}$	$0.456 \cdot 10^{-8}$
	τ_y	$0.444 \cdot 10^{-8}$	–	$0.444 \cdot 10^{-8}$

Values in Tables 3 and 6 indicate, that errors in stresses yielding from the solution to the Dirichlet boundary value problem obtained with extended precision are about 10^7-times smaller than for single precision.

Assessment of accuracy of numerical results is subjective and depends on the goal of computations. For instance, in the scale of Figs. 6*a* – 11*a* the smoothed solutions, both in single and extended precision, can be considered as satisfactory. If there is a need for more precise analyses, smoothed solutions obtained from extended precision are numerically correct.

8. CONCLUSIONS

This paper addressed a question of numerical errors occurring in the finite difference method applied to solve equations of the theory of elasticity describing a two-dimensional adhesive joint in a plane stress state. The formulation was expressed in displacements by means of a set of four partial differential equations of the second order with static and kinematic boundary conditions. Static boundary conditions involved loading applied to the joint, while the kinematic ones – constraining of adherends resulting in a geometrically stable system.

Solutions to the problem expressed in displacements, yielding from the finite difference method, are sensitive to kinematic boundary conditions. It can be observed when adhesive joint is constrained in a statically determinate way and loading is self-equilibrated. Then reactions at constraints should be equal to zero but the finite difference solution does not meet this condition accurately. Thus, the solution is erroneous and the adhesive joint behaves as if it was not in

an equilibrium state. Here this phenomenon was called *numerical non-equilibrium.*

The numerical non-equilibrium results in a small asymmetry and local concentrations at constraining points of adhesive joints. The magnitude of local disturbances in the solutions depends strongly on precision of computations.

Numerical examples presented in Section 5 illustrate this phenomenon sufficiently for the displacement formulation of the problem. The numerical non-equilibrium is observed in all the cases of adhesive joints constrained in a statically determinate way and the joints are under a self-equilibrated loadings.

Disturbances in displacements and, consequently, in stress distributions resulting from constraining of an adhesive joint can be decreased or eliminated by a correction of loading. This correction can take many forms but every type of such a correction will violate the equilibrium of the original system. Such an approach requires numerous computations and does not lead to a unique solution. *Smoothing of solutions* is a more appropriate method.

The method of solution smoothing proposed in this paper is based on an observation, that the influence of local disturbances in displacements is limited to small zones on an adhesive surface around constraining points. Thus, if a constraining point is sufficiently remote from the adhesive edges, then a local disturbance in displacements has a negligible effect on displacements values at points located at the adhesive edges.

The smoothing method involves two subsequent solutions to two different boundary value problems for the same adhesive joint. In the first problem displacements fulfilling static and kinematic boundary conditions are found. As a result displacements functions for adherends are found and they are defined on the entire adhesive surface including the displacements at adhesive edges. If constraining points are sufficiently remote from the adhesive edges, then the functions of displacements for edge points are free of errors resulting from the numerical non-equilibrium, as was confirmed by a solution of the problem expressed in stresses, which is independent of kinematic boundary conditions. The displacement functions as given continuous functions on the edges of the definition set of the differential equations can be adopted as boundary functions for the second boundary value problem, i.e. the Dirichlet one. Such an approach proved to be very efficient numerically, what results from the stability of the finite difference method for elliptic differential equations.

The difficulties with numerical non-equilibrium and solutions smoothing do not occur, if an adhesive joint is supported in a statically indeterminate way or

loading is not self-equilibrated. Then reactions at the supports are non-zero, not due to any numerical error, but due to equilibrium conditions and kinematic equivalence of the adhesive joint as an externally statically indeterminate system. Those solutions are subjected to numerical errors but their magnitudes are negligible, especially in the case of extended precision computations.

The phenomenon of numerical non-equilibrium and the proposed method of solutions smoothing, presented in an example of a mathematical model of two-dimensional adhesive joints, can be used in many other problems involving numerical solutions to boundary value problems with differential equations.

REFERENCES

1. Andermann F.: *Tarcze prostokątne. Obliczenia statyczne*, Warszawa, Arkady 1966.
2. Cea J.: *Approximation variationelle des problemes aux limites*. Ann. Inst. Fourier, Grenoble, 14 (1964), 345–388.
3. Collatz L.: *Numerical solutions to differential equations Numerische Behandlung von Differentialgleichungen*, Berlin-Göttingen-Heidelberg, Springer-Verlag 1953.
4. Dankert J.: *Numerische Methoden der Mechanik*, VEB Fachbuchverlag, Leipzig 1977.
5. Fichera G.: *Existence Theorems in Elasticity* [in:] *Encyclopedia of Physics*, Vol. VIa/2 *Mechanics of Solids II*. ed. Truesdell C., Springer-Verlag 1972.
6. Forsythe G.E., Wasow W.R.: *Finite – difference methods for partial differential equations*, John Wiley & Sons, Inc. 1960.
7. Fung Y.C.: *Foundations of solid mechanics*, Prentice-Hall, Inc. 1965.
8. Girkmann K.: *Plane girders Flächentragwerke*, Wien, Springer-Verlag 1956.
9. Huber M. T.: *Teoria sprężystości*, część I, Warszawa, PWN 1954.
10. Korn A.: *Sur les équation de l' élasticité.* Annales de l'école normale supérieure, 1907.
11. Krzyżański M.: *Partial differential equations of second order*, vol. I. Monografie Matematyczne, tom 53, Warszawa, PWN 1971.
12. Lapidus L., Pinder G.F.: *Numerical solution of partial differential equation in science and engineering*, John Wiley & Sons, INC. 1982.
13. Love A.E.H.: *A Treatise on the Mathematical Theory of Elasticity*, Cambridge at the University Press 1959.
14. Marcinkowska H.: *Wstęp do teorii równań różniczkowych cząstkowych*, Biblioteka Matematyczna tom 43, Warszawa, PWN 1972.

15. Nowacki W.: *Teoria sprężystości*, Warszawa, PWN 1970.
16. Orkisz J.: *Metoda różnic skończonych*. [w:] Kleiber M. (red.): *Mechanika techniczna, tom IX. Komputerowe metody mechaniki ciał stałych*, Warszawa, PWN 1995, 346–398.
17. Petrowski I. G.: *Lectures on Partial Differential Equations*, Wiley-Interscience, 1954.
18. Rapp P.: *Mechanika połączeń klejowych jako płaskie zadanie teorii sprężystości*, Politechnika Poznańska, Rozprawy nr 441. Wydawnictwo Politechniki Poznańskiej, Poznań 2010.
19. Rapp P.: *Mechanics of adhesive joints as a plane problem of the theory of elasticity. Part I: General formulation*, Archives of Civil and Mechanical Engineering, 10, 2 (2010) 81-108.
20. Rapp P.: *Mechanics of adhesive joints as a plane problem of the theory of elasticity. Part II: Displacement formulation for orthotropic adherends*. Archives of Civil and Mechanical Engineering, 15, 2 (2015) 603-613.
21. Rapp P.: *Stress equations for adhesive in two-dimensional adhesively bonded joints*, Civil and Environmental Engineering Reports, 14, 3 (2014) 75-94.
22. Sokołowski M. (red.): *Mechanika techniczna, tom IV. Sprężystość*, Warszawa, PWN 1978.
23. Timoshenko S., Goodier J. N.: *Theory of elasticity*, McGraw-Hill Book Company, Inc. 1951.

NIERÓWNOWAGA NUMERYCZNA I WYGŁADZANIE ROZWIAZAŃ W METODZIE RÓŻNICOWEJ DLA DWUWYMIAROWYCH POŁĄCZEŃ KLEJOWYCH

S t r e s z c z e n i e

Przedmiotem pracy są błędy numeryczne metody różnicowej zastosowanej do rozwiązania równań teorii sprężystości opisujących dwuwymiarowe połączenia klejowe w płaskim stanie naprężenia. Połączenia klejowe opisane są w przemieszczeniach za pomocą układu czterech eliptycznych równań różniczkowych cząstkowych rzędu drugiego z warunkami brzegowymi statycznymi i kinematycznymi. Jeśli połączenie klejowe jest unieruchomione w sposób statycznie wyznaczalny i jest obciążone zrównoważonym układem obciążeń, to rozwiązania różnicowe są wrażliwe na kinematyczne warunki brzegowe. W punktach unieruchomienia takiego połączenia przemieszczenia nie są dokładnie równe zeru. Rozwiązanie różnicowe jest obarczone błędem numerycznym, w wyniku którego połączenie klejowe zachowuje się tak, jakby

nie było w równowadze. Zjawisko to w tej pracy określa się terminem *nierównowaga numeryczna.* Zaburzenia rozkładów przemieszczeń i naprężeń można zmniejszyć lub usunąć za pomocą korekty obciążeń działających na połączenie klejowe lub przez *wygładzenie rozwiazań* bazujące na zadaniu brzegowym Dirichleta

Słowa kluczowe: połączenie klejowe, liniowa teoria sprężystości, metoda różnic skończonych, błąd numeryczny, wygładzanie rozwiązań, zadanie brzegowe Dirichleta

Editor received the manuscript: 24.05.2015